Evidence of Accumulating Neurophysiologic Dysfunction in Persistent Post-COVID Fatigue

Maria Germann[1], Natalie J. Maffitt[2], Olivia A. Burton[1], Amn Ashhad[1], Anne M.E. Baker[2], Boubker Zaaimi[3], Wan-Fai Ng[1,4,5], Demetris S. Soteropoulos[2], Stuart N. Baker[2] and Mark R. Baker[1,6]

[1] Translational and Clinical Research Institute, Faculty of Medical Sciences, Newcastle University, Newcastle Upon Tyne NE2 4HH, Tyne and Wear, UK

[2] Biosciences Institute, Faculty of Medical Sciences, Newcastle University, Newcastle upon Tyne NE2 4HH, Tyne and Wear, UK

[3] College of Health and Life Sciences, Aston University, Birmingham B4 7ET, UK

[4]Rheumatology department, Cambridge University Hospitals NHS Foundation Trust, Cambridge, UK

[5]College of Medicine and Health, University College Cork, Cork, Ireland, UK

[6]Clinical Neurosciences, Newcastle upon Tyne Hospitals NHS Foundation Trust, Royal Victoria Infirmary, Queen Victoria Rd, Newcastle upon Tyne, NE1 4LP, UK

Abstract

A major consequence of the COVID-19 pandemic has been the emergence of post-COVID syndrome (PCS), and more specifically, post-COVID fatigue (pCF), with an estimated prevalence of ~2%. We previously showed that, compared to healthy controls, people with pCF exhibit changes in muscle physiology, cortical circuitry, and autonomic function.

Here we present results from a cohort of people with pCF (N=145), between 12 weeks and 45 months post-infection. We report self-perception of fatigue; objective measures of cortical circuits via transcranial magnetic stimulation and reaction time tasks; peripheral muscle fatigue; and autonomic function such as heart rate variability.

Those with pCF persisting >200 days had significantly more fatigue and showed increased cortical excitability, slower reaction times and increased peripheral muscle fatigue compared to those with <200 days of pCF .

In pCF, if there is no spontaneous recovery, fatigue worsens, and patients continue to accumulate significant neurophysiologic abnormalities.

Introduction

Since the onset of the COVID-19 pandemic, it has become increasingly evident that a small but significant proportion of individuals experience persistent symptoms beyond the acute infection, a condition now widely referred to as long COVID or post-COVID syndrome (PCS). PCS is defined by the National Institute for Care and Excellence (NICE) as symptoms that exist three months after the acute infection[1], and currently affects ~2% of the UK population[2].

Among the broad range of symptoms associated with PCS, fatigue is one of the most frequently reported and most disabling. In the United Kingdom, post-COVID fatigue (pCF) affects 71% of those with long COVID[2], contributing to reduced occupational participation, diminished quality of life, and increased demand on healthcare services. The scale of this burden, combined with the heterogeneity of its presentation and the absence of specific diagnostic tools, underscores the urgency of understanding the biological underpinnings and clinical course of fatigue in this context.

Fatigue in PCS is multifactorial, encompassing not only overwhelming feelings of tiredness, but also cognitive/mental fatigue frequently described as "brain fog"[3] and disproportionate symptom exacerbation after minimal exertion (post-exertional malaise)[4]. Reports also highlight muscle weakness, myalgia, and impaired motor coordination among long COVID patients[5-7], indicating lasting muscle pathology even in individuals with a history of mild COVID-19[8-10]. The underlying mechanisms of pCF remain incompletely understood with hypotheses including immune dysregulation[11], autonomic nervous system dysfunction[12], mitochondrial impairment[10], and psychosocial contributors[13].

The severity and pattern of fatigue can vary widely between individuals, and its course may fluctuate over time. Some patients report gradual improvement or even complete remission[14]; others have persistent or relapsing fatigue over months to years.

To understand the clinical, biological and social dimensions of pCF, longitudinal studies are crucial. These allow for the identification of distinct trajectories and predictors of recovery or chronicity, by documenting clinical and physiological changes over time.

In a previous study[15] comparing individuals with pCF to a healthy control cohort, we identified changes in physiology relating to dysautonomia, cortical excitability and muscle pathology. A

subset of the same pCF cohort was then followed after 6 and 12 months[16]. As a cohort, most neurophysiological metrics as well as self-reported perception of fatigue significantly improved, slowly returning to levels seen in healthy controls. However, some individuals continue to suffer from post-COVID fatigue two or more years after their initial infection.

Here we take a larger cohort of individuals suffering from pCF after non-severe SARS-CoV-2 infection and demonstrate that neurophysiological measurements differ depending on the duration of pCF. We provide evidence that pCF is initially characterised by autonomic dysregulation, peripheral muscle pathology and reduced cortical excitability, in line with our previous results[15]. Over time, the neurophysiologic abnormalities evolve, with progressive changes in measures of cortical excitability and processing, as well as increasing peripheral muscle fatigue. By contrast, measures of autonomic function appear unchanged regardless of time since infection.

Methods

Participants

The study was approved by the Ethics Committee of Newcastle University Faculty of Medical Sciences. Participants provided written informed consent.

For this study, data from 145 participants (108 females) who were suffering from pCF by self-report were analysed. This included data from a pCF cohort of 37 participants (27 females) that were collected for our previous studies[15,16] and baseline data (prior to any intervention) from individuals with pCF (108 participants, 81 females) that went on to participate in a vagus nerve stimulation trial (ISRCTN registry; ISRCTN18015802). For the electrophysiological tests, the previous cohort of 52 healthy volunteers (37 females) with no symptoms of fatigue served as the control dataset[15,16]. In this control cohort, six subjects had reported having mild COVID-19 but with complete recovery and no symptoms of pCF.

All participants were 18-65 years of age and had no history of neurological disease.

For the purposes of this study, pCF participants were divided according to their time since infection (time of suffering from pCF), leading to two distinct groups: less than 200 days since

115 COVID-19 infection (N=44; 31 females) and more than 200 days since infection (N=101; 77
116 females).

117 Figure 1 shows the time since infection for each individual in the pCF cohort.

118 Questionnaires

119 The Fatigue Impact Scale (FIS) was used to quantify subjective levels of fatigue. The FIS has 40
120 questions in total, evaluating the effect of fatigue on three domains of daily life: cognitive,
121 physical and psychosocial functioning[17].

122 A subset of 109 pCF participants also filled out a Fatigue Visual Analogue Scale, which simply
123 asked them to score their fatigue that day on a scale from 0 (no fatigue) to 100 (extreme
124 fatigue).

125 General Electrophysiological Methods

126 The assessment protocols follow our previous studies[15,16] which compared participants with
127 pCF to age-matched controls and followed a cohort of pCF participants for a year. A summary
128 of the various electrophysiological measures is illustrated in Figure 2.

129 Electromyogram (EMG) was recorded through adhesive surface electrodes placed on the skin
130 over the muscle belly. EMG signals were amplified and filtered (band-width 30-2000 Hz) with
131 a bioamplifier (D360 8-Channel Patient Amplifier, Digitimer, Welwyn Garden City, UK) and
132 then converted to digital data with a sampling rate of 5kHz (CED Micro 1401 with Spike2
133 software, Cambridge Electronic Design, Cambridge, UK) and stored on a computer for off-line
134 analysis. Where a measurement required a constant contraction, visual feedback of rectified
135 and smoothed EMG activity was provided to the subject via a display of coloured bars on a
136 computer screen, calibrated to the subject's maximum voluntary contraction (MVC).
137 Participants were then asked to maintain a contraction corresponding to 10% of their
138 individual MVC. Transcranial magnetic stimuli were applied using a figure-of-eight coil
139 through a Bistim 200^2 stimulator (Magstim, Whitland, UK). The magnetic coil was held to
140 induce electrical currents that flow perpendicular to the presumed line of the central sulcus
141 in a posterior-anterior direction, with the handle pointing posteriorly and 45° away from the
142 midline. The hotspot was defined as the region where the largest motor-evoked potential
143 (MEP) in the target muscle could be evoked. To ensure a stable coil position during
144 experiments and across sessions, the site of stimulation was marked using a Brainsight

145 neuronavigation system (Rogue Research Inc., Montréal, Canada), which allows online
146 navigation. A Polaris Vicra camera (Northern Digital Inc., Canada) was used to track the coil.

147 ## Peripheral nerve stimulation

148 Stimuli to peripheral nerves (0.2 ms pulse width) were delivered using a Digitimer DS7AH
149 isolated, constant current stimulator. The size of the maximal M wave was measured by
150 stimulating the median nerve at the wrist and recording EMG from the abductor pollicis brevis
151 (APB) muscle. Stimulus intensity was set to produce a supra-maximal M wave. Ten stimuli at
152 this intensity were delivered and the highest amplitude M wave was used for subsequent
153 normalisation of TMS recruitment curves (see below).

154 ## TMS recruitment curve

155 As a measure of motor cortical excitability, the increase in APB MEP with increasing stimulus
156 intensity was used[18]. The active motor threshold (AMT) was defined as the intensity which
157 produces a MEP > 100 µV amplitude in at least 3 out of 6 stimuli, while the participant
158 maintained an active contraction of 10% MVC. The intensity of the stimulation was expressed
159 as a percentage of the maximal stimulator output (MSO). Recruitment curves of increasing
160 intensities in 10% MSO steps were obtained in blocks of ten stimuli per step starting at AMT
161 intensity, until 100% MSO was reached.

162 Offline analysis measured the size of MEPs from single trials and plotted this versus stimulus
163 intensity. A sigmoid curve could then be fitted to the relationship[19].

164 ## Paired-pulse TMS

165 The hotspot was defined as the region where the largest MEP in the first-dorsal interosseous
166 (1DI) muscle could be evoked with the minimum intensity. Resting motor threshold (RMT)
167 was defined as the minimal stimulus intensity needed to produce a MEP > 100 µV amplitude
168 in at least 3 out of 6 stimuli.

169 For the test stimulus, TMS intensity was adjusted to elicit MEPs of 1mV amplitude at rest, or
170 to 120% RMT, whichever was lower. The conditioning stimulus intensity was set at 80% RMT.

171 Conditioning stimuli preceded the test stimuli by 3 or 10 ms and the recorded responses were
172 compared to responses to the test stimulus alone, to measure short-interval intracortical
173 inhibition (SICI) and intracortical facilitation (ICF) respectively Kujirai, et al. [20]. Twenty stimuli

for each condition were given in a pseudo-random order. Responses to the conditioning stimuli were expressed as a percentage to the responses to the test stimulus alone.

Galvanic skin response

The galvanic skin response (GSR) is a measure of the cutaneous resistance or conductivity, which can be quantified by passing a weak electric current through a pair of electrodes. Variation in skin resistance depends on sweat production, which itself is mediated by the sympathetic system[21]; its habituation may be a relevant measure in assessing cognitive states[22]. The GSR was measured by placing two metal plates on the lateral and medial surfaces of the index finger. Five loud sounds (115 dB, C weighting, 500Hz, 50 ms, 8-8.8s inter-stimulus interval, chosen randomly from a uniform distribution) were played through loudspeakers placed underneath the subject chair, with the subject at rest. The ratio of the GSR response amplitude following the last stimulus compared to the first was used as a measure of habituation.

StartReact effect

This paradigm measures reaction time from EMG in response to a visual cue (visual reaction time, VRT), a visual plus quiet auditory cue (visual-auditory reaction time, VART), and a visual plus loud auditory cue (visual-startle reaction time, VSRT). The acceleration of reaction time between VART and VSRT is termed the StartReact effect and has previously been used to assess connections from the reticulospinal system[23-26].

A green light-emitting diode (LED) was located ~1 m in front of the subject. Participants were instructed to flex their elbow and clench their fist as quickly as possible after the LED illuminated. EMG was recorded from both the first dorsal interosseous muscle (1DI) and biceps muscle, and reaction time measured as the time from cue to onset of the EMG burst. Three types of trial were randomly interleaved (20 repeats per condition; inter-trial interval 6-6.8s, interval chosen randomly from a uniform distribution): LED illumination alone (VRT), LED paired with a quiet sound (80dB, 500Hz, 50ms, VART), LED paired with a loud sound (500 Hz, 50ms, 115 dB, VSRT).

StartReact measurements were performed immediately after the GSR Habituation test, ensuring that any overt startle reflex had been habituated by the five loud sounds given in that test. The room lights were dimmed for this test.

Data were analysed offline trial-by-trial using a custom MATLAB program which identified the reaction time as the point where the rectified EMG exceeded the mean + 7 SD of the baseline measured 0-200 ms prior to the stimulus. Every trial was also inspected visually, and erroneous activity onset times (caused, for example, by electrical noise artefacts) was manually corrected. Average VRT, VART and VSRT were calculated for each subject and muscle, together with the amplitude of the StartReact effect, equal to VSRT-VART.

Stop-signal reaction time

The stop-signal reaction time (SSRT) task measures the ability to inhibit a response after receiving a go cue. Participants are asked to respond to a go cue, but to inhibit their responses if a stop cue appears. This can indicate the state of premotor cortical-subcortical areas involved in impulse control[27] and test for increased levels of inhibition in the motor system. SSRT was measured with a recently-developed portable device that uses Bayesian statistical analysis to improve the reliability of the measure[28]. The battery-powered device consisted of a plastic box which contained a microcontroller and a LCD screen, as well as one green LED, one red LED and a press button. Participants initiated a trial by pressing and holding down the response button. They were instructed to release this button as quickly as possible when the green LED was illuminated (GO trial; 75% of trials).

On 25% of trials, the red LED illuminated 5, 65, 135 or 195ms after the green LED (stop trial) and participants were instructed not to release the button on these trials. Trials were presented in three blocks of 64, with a 60 s break between each block. Each block consisted of 48 GO trials and 16 STOP trials (four for each delay). Using the distribution of reaction times on the GO trials, and the proportion of successfully inhibited responses, the algorithm calculated the SSRT as described in full in our previous work[28].

Electrocardiogram

A single channel of electrocardiogram (ECG) recording was captured, using a differential recording from left and right shoulder (bandpass 0.3-30 Hz) and stored for offline analysis. The time of each QRS complex was extracted. From these times, the mean heart rate and the pNN50 (a measure of heart rate variability and defined as the proportion of successive intervals which differ by >50ms) were computed. ECG was captured while participants were engaged in the SSRT test (see above), to ensure consistent behaviour across recordings.

Twitch interpolation

Our previous studies[15,16] used the twitch interpolation procedure, which allows assessment of an individual's ability to activate a muscle voluntarily maximally, before and after a sustained (fatiguing) contraction. The experimental sequence followed previous work from this laboratory, to ensure that measurements would be comparable.

Subjects sat with their arm and forearm strapped into a dynamometer to measure torque about the elbow. The forearm was held vertically in supination, the upper arm horizontal and the elbow was flexed at a 90° angle. Velcro straps held the wrist, forearm and upper arm in place. Thin stainless-steel plate electrodes (30 x 15 mm) covered in saline-soaked gauze were used for electrical stimulation of the biceps muscle, by taping one electrode over the muscle belly and one over its distal tendon. The individual supramaximal stimulus level was set by increasing the intensity until the twitch response (recorded by the dynamometer) grew no further.

Upon receiving an auditory cue, subjects performed a 3s long maximal voluntary contraction until a stop tone sounded. Electrical stimulation to the biceps was given during MVC, 2s after the go cue and at rest, 5s after the stop cue. This sequence was repeated twice, with a 60 s rest period between go cues. After another 60s rest, another go cue then indicated to the subject to make a sustained MVC of up to 90s. If exerted force fell below 60% of the initial maximal level, contraction was terminated early. During this long MVC, the biceps muscle was stimulated every 10s. A final three stimuli (inter-stimulus interval 5s) were given at rest.

If a subject truly performs a maximal voluntary contraction, a superimposed electrical stimulus should not be capable of generating extra force. The size of any elicited twitch thus measures a central activation deficit. Stimulation of a fatigued muscle at rest after the long contraction produces a smaller twitch than that seen before the sustained MVC, indicating peripheral fatigue.

Central activation before and after fatigue, as well as peripheral fatigue were computed based on elicited twitches according to the calculations inMcDonald, et al. [29].

Biometric Data

Various biometric measurements were collected from participants. These included blood oxygen saturation using a pulse oximeter placed onto the index finger, tympanic temperature,

height, weight and full body composition (BC-545N Segmental Body Fat Scale, Tanita, Amsterdam, The Netherlands).

Analysis

Data processing and statistical analyses were conducted using MATLAB (The MathWorks, Inc., Natick, MA, USA), SPSS (IBM SPSS Statistics for Windows, Armonk, NY: IBM Corp) and R (http://www.r-project.org/).

Descriptive statistics are given as mean ± standard deviation. Because each measure has different units and scales, data were normalized as a Z-score to allow easy comparison of differences. Z-scores were calculated by taking the difference in means of a measure between datasets (pCF vs healthy controls or pCF less than vs greater than 200 days) and dividing it by the standard deviation of the normative dataset (healthy controls or pCF less than 200 days). This is a measure of effect size and similar to Hedge's g measure.

For the distribution of Z scores across subjects with similar times since infection, the sum of Z scores across all measures were taken for each subject. Subjects were ordered in ascending order according to their time since infection (most recently infected to longest time since infection) and groups of 20 subjects were taken to contribute to the overall sum of Z score for that bin, starting with the 20 most recently infected people. Each bin was moved by one subject at a time until the last bin included the 20 subjects that had pCF for the longest. If participants did not have a measure, the missing data was substituted by the mean of the Z scores across all subjects for that measure. For the sum of Z scores to reflect overall symptom burden, the signage of measures where the mean of the pCF cohort was smaller than the mean of the healthy control cohort was flipped (multiplied by -1), so that a higher Z score always reflected a larger distance from healthy for all measures.

To compare the cohorts (pCF vs healthy controls or the two separate pCF cohorts), unpaired t-tests were used. The Benjamini-Hochberg procedure was used to correct for multiple comparisons[30]. Raw (uncorrected) P-values are given throughout this report, but only stated as significant if they passed correction for multiple comparisons.

The correlation coefficient is given as Pearson's r.

Results

Comparing Post-COVID Fatigue and Healthy Controls

Measures from all participants suffering from post-COVID fatigue (N=145; 108 female; 48.2 ± 9.8 years) were compared with a healthy control cohort (N=52; 37 females; 46.6 ± 9.4 years). Figure 3 illustrates results for all electrophysiological measures as a spider plot[31], normalized as Z-scores and ordered so the greatest difference is located at the top of the figure. P-values are listed in Table 1.

Our results are largely consistent with our previously reported study comparing the same control cohort to a smaller subset of the pCF cohort used here[16]. For this present study we found several more metrics to be significantly different between patients with pCF and controls. This is most likely due to the increased number of subjects and the notably longer time this cohort had been suffering from the condition (505 ± 339 days since infection compared to 121 ± 37 days since infection for the previous cohort [16]).

Multiple TMS measures related to cortical excitability were significantly different between the healthy control cohort and the pCF cohort (resting motor threshold *TMS_RMT* p<0.001, active motor threshold *TMS_AMT* p<0.001, the asymptote of the recruitment curve normalized to M-max *TMS_Asymptote_Norm* p=0.031, the intensity yielding 50% of the asymptote response amplitude *TMS_I50* p=0.0103, active motor threshold of the cortical silent period *TMS_CSP_AMT* p<0.001 and I50 of the cortical silent period *TMS_CSP_I50* p=0.0133).

The recruitment curve slope (*TMS_Slope* p=0.385), the asymptote of the recruitment curve (*TMS_Asymptote* p=0.130) and the recruitment curve slope of the cortical silent period (*TMS_CSP_Slope* p=0.782) were not significantly different between cohorts. Additionally, intracortical facilitation was significantly decreased in pCF patients (*ICF* p<0.001), but short-interval intracortical inhibition did not show a difference between patients with pCF and controls (*SICI* p=0.725).

We found longer reaction times in pCF versus controls for all measures relating to the StartReact paradigm in both muscles (visual reaction time *STR_VRT_Bic* p<0.001 and *STR_VRT_1DI* p<0.001, visual-auditory reaction time *STR_VART_Bic* p<0001 and *STR_VART_1DI* p<0.001, visual-startle reaction time *STR_VSRT_Bic* p<0.003 and

322 *STR_VSRT_1DI* p<0.001). The StartReact effect, which measures the acceleration of a visual
323 reaction time by a loud (startling) sound and has been proposed to assess reticulospinal
324 pathways[32], was also significantly increased in both muscles (*STR_StartReact_Bic* p<0.001 and
325 *STR_StartReact_1DI* p=0.009), while the difference between visual reaction time and visual-
326 auditory reaction time was reduced in pCF versus controls (*STR_Multisense_1DI* p=0.0171)
327 but did not pass correction for multiple comparisons in the biceps muscle
328 (*STR_Multisense_Bic* p=0.042). The stop-signal-reaction time (*SSRT_ocSSRT* p=0.614) was the
329 same for both cohorts.

330 We also found evidence of autonomic dysregulation in the pCF group, showing lower
331 peripheral blood oxygen saturation (*pO2* p<0.001), lower galvanic skin response habituation
332 (*GSR_Habituation* p=0.022), increased resting heart rate (*Mean_HR* p=0.003) and lower heart
333 rate variability (*pNN50* p<0.001, *HR_RMSSD* p=0.007, *HR_SDNN* p=0.004). Other measures of
334 autonomic function (tympanic temperature *Temp* p=0.272 and variability in heart rate
335 coefficient of variation *HR_CV* p=0.305) did not differ between cohorts.

336 Maximal voluntary contraction (*TI_MVC* p=0.090) was not significantly reduced in pCF,
337 suggesting no deficit in force production for brief contractions. There also was no difference
338 in maximal M-wave (*Mmax* p=0.919), or their maximal elicited muscle twitch (*TI_TwitchMax*
339 p=0.838). However, after a prolonged maximal contraction, pCF participants had an increased
340 level of peripheral fatigue (size of maximum twitch evoked by direct electrical stimulation of
341 the muscle after a sustained contraction compared with baseline; *TI_PeriphFatigue* p<0.001).

342 Central activation, which assesses the ability of the CNS to activate muscle maximally
343 voluntarily, was significantly reduced in pCF, either assessed at baseline (*TI_CA_baseline*
344 p=0.002) or after a fatiguing contraction (*TI_CA_fatigue* p<0.001).

345 In terms of body composition, pCF participants weighed significantly more (*Scales_Weight*
346 p<0.001), but their body weight actually consisted of more muscle mass (*Scales_Muscle*
347 p<0.001) and less fat by percentage (*Scales_Fat* p<0.001), whereas there was no difference in
348 water mass by percentage (*Scales_H2O* p=0.045, not significant after correcting for multiple
349 comparison) between the cohorts.

Changes in Physiology over time

Sum of Z Scores Distribution

To assess physiological differences over time, a sum of Z scores across all measures was calculated for each subject. Subjects were ordered in ascending order according to their time since infection (most recently infected to longest time since infection) and bins of 20 subjects were taken to contribute to the overall sum of Z score for that bin, starting with the 20 most recently infected people. Each bin was moved by one subject at a time until the last bin included the 20 subjects that had pCF for the longest. Figure 4A illustrates sum of Z scores for these bins over time, with time since COVID for each bin being the average time since infection across the 20 people in that bin.

The sum of Z rises steeply between 90 and 360 days since infection, indicating an increase in physiological differences compared to healthy controls over that time period. From 360 days to 800 days since infection, the sum of Z then drops about halfway before rising again to similar levels as the peak at 360 days. The midpoint of the rising curve (grey dotted lines in Figure 4A) was determined as 200 days since COVID infection. We chose this cut off point, because all bins with more than 200 days since COVID have higher sum of Z than those with less than 200 days since COVID.

Figure 4B validates the sum of Z scores as a measure of overall symptom burden by illustrating its distribution among the healthy control cohort and the pCF cohort. While there is some overlap between the two cohorts, the pCF cohort shows a clear shift towards higher sums of Z scores across measures ($p<0.001$).

Differences in Individuals Before and After 200 Days of Post-COVID Fatigue

Participants were split into two groups according to their time since infection. The first group contained people that had pCF for less than 200 days (N=44; 31 females; 46.7 ± 9.1 years) and the second group contained people that had pCF for over 200 days (N=101; 77 females; 48.8 ± 10.1 years). We refer to these groups below using the shorthand pCF<200 and pCF>200.

Measures that were significantly different between pCF and the control cohort (Figure 3) were compared with unpaired t-tests between pCF<200 and pCF>200. Figure 5 illustrates results for these electrophysiological measures as a spider plot[31], normalized as Z-scores and ordered so the greatest difference is located at the top of the figure. P-values are listed in Table 1.

381 pCF>200 participants reported significantly higher levels of fatigue according to the Fatigue
382 Impact Scale compared pCF<200 (*FIS_Total* pCF<200 85.5 ± 25.8, pCF>200 100.0 ± 25.4,
383 p=0.002). pCF>200 scored notably higher on all FIS subscores (*FIS_Social* pCF<200 38.8 ± 13.7,
384 pCF>200 46.6 ± 14.3, p=0.003; *FIS_Physical* pCF<200 24.8 ± 5.6, pCF>200 27.8 ± 6.0, p=0.006;
385 *FIS_Cognitive* pCF<200 21.9 ± 8.7, pCF>200 25.6 ± 7.6, p=0.011).

386 pCF>200 also had higher peripheral muscle fatigue (*TI_PeriphFatigue* p=0.009) and a lower
387 body fat percentage (*Scales_Fat* p<0.001).

388 Importantly, all other measures that were significantly different between pCF<200 and
389 pCF>200 assessed the central nervous system. These included TMS measures showing
390 increased cortical excitability in pCF>200 (*TMS_AMT* p<0.001; *TMS_RMT* p<0.001; *TMS_I50*
391 p<0.001; *TMS_CSP_AMT* p<0.001; *TMS_CSP_I50* p<0.001; *SICI_1mV_MEP* p<0.001),
392 significantly slower reaction times in pCF>200 (*STR_VART_1DI* p=0.010; *STR_VSRT_Bic*
393 p=0.015; *STR_VSRT_1DI* p=0.021; *STR_Multisens_1DI* p=0.003) and a larger central activation
394 deficit in pCF>200 (*TI_CA_Fatigue* p=0.006; *TI_CA_Baseline* p=0.018).

395 Correlating neurophysiological measures with time since infection (Supplementary Table 1),
396 we found significant correlations for measures of cortical excitability (*TMS_AMT, TMS_RMT,*
397 *TMS_1mV_MEP, TMS_I50, TMS_asymptote, TMS_CSP_AMT* and *TMS_CSP_I50*; all p<0.001).

398 On the other hand, measures assessing autonomic function of the nervous system seemed to
399 be similar between pCF<200 and pCF>200 (*Mean_HR* p=0.060; *HR_RMSSD* p=0.347;
400 *HR_SDNN* p=0.489; *pNN50* p=0.505; *GSR_Habituation* p=0.786; pO_2 p=0.918). There was also
401 no difference in intracortical facilitation (*ICF* p=0.353), or in body weight and muscle
402 percentage (*Scales_Weight* p=0.064; *Scales_Muscle* p=0.306) and some measures of reaction
403 time such as the StartReact effect were also similar (*STR_StartReact_Bic* p=0.462;
404 *STR_StartReact_1DI* p=0.525; *STR_VRT_Bic* p=0.163; *STR_VRT_1DI* p=0.252).

405 More evidence that people suffering from pCF for over 200 days deteriorate physiologically
406 comes from comparing each pCF cohort to healthy controls separately (Figure 6). Figure 6A
407 compares pCF<200 with healthy controls; only 8 measures out of 42 showed a significant
408 difference (P-values are listed in Table 1). These measures included those which we previously
409 reported to be different between healthy controls and pCF[16], including intracortical
410 facilitation (*ICF* p=0.001), mean resting heart rate (*Mean_HR* p=0.015), peripheral muscle

411 fatigue (*TI_PeriphFatigue* p=0.007) and blood oxygen (*pO_2* p<0.001). Additionally, here we
412 also found reduced heart rate variability (*HR_RMSSD* p=0.007; *pNN50* p=0.008) and a
413 difference in body composition (*Scales_Muscle* p<0.001; *Scales_Weight* p<0.001).

414 When comparing pCF>200 with healthy controls (Figure 6B), it became evident that they
415 deviated more from healthy controls, with 31 out of 42 measures being significantly different.
416 P-values are listed in Table 1.

417 In pCF>200, two more measures relating to autonomic function were significantly different
418 from healthy controls (*GSR_Habituation* p=0.021; *HR_SDNN* p=0.012) in addition to the four
419 measures of the group with pCF for a shorter time (*pO_2* p<0.001; *Mean_HR* p=0.018;
420 *HR_RMSSD* p=0.027; *pNN50* p<0.001). This pCF cohort also showed a central activation deficit
421 (*TI_CA_Fatigue* p<0.001; *TI_CA_Baseline* p<0.001) as well as the peripheral muscle fatigue
422 (*TI_PeriphFatigue* p<0.001) already present in the more recently infected cohort. There were
423 more changes in body composition (*Scales_Fat* p<0.001; *Scales_H_20* p=0.006; as well as
424 *Scales_Muscle* p<0.001; *Scales_Weight* p=0.004). In addition to increased cortical facilitation
425 (*ICF* p<0.001) this cohort showed changes in a multitude of measures assessing cortical
426 excitability (*TMS_CSP_AMT* p<0.001; *TMS_AMT* p<0.001; *TMS_RMT* p<0.001; *TMS_CSP_I50*
427 p<0.001; *TMS_I50* p<0.001; *SICI_1mV_MEP* p<0.001; *TMS_asymptote_norm* p=0.024). Lastly,
428 people that had pCF for over 200 days also had decreased reaction times compared to healthy
429 controls (*STR_VART_1DI* p<0.001; *STR_VART_Bic* p<0.001; *STR_Multisens_1DI* p<0.001;
430 *STR_VSRT_1DI* p<0.001; *STR_VRT_1DI* p<0.001; *STR_Startreact_Bic* p<0.001;
431 *STR_Multisens_Bic* p<0.001; *STR_VRT_Bic* p<0.001; *STR_VSRT_Bic* p<0.001;
432 *STR_StartReact_1DI* p=0.003), which was not seen in people that had pCF for less than 200
433 days.

434

435 ## Discussion

436

437 Long COVID has emerged as a debilitating and common complication of the COVID-19
438 pandemic, which can affect people even after a mild initial infection. Studies indicate that
439 approximately 10-20% of people infected with SARS-CoV-2 continue to experience long-term
440 sequelae up to six months after the acute infection[33,34]. In the UK, an estimated 3.1% of the

441 population were experiencing persistent symptoms after a COVID infection[2]. While some
442 individuals affected by post-COVID syndrome will spontaneously recover, there is currently
443 no clear treatment for the condition and many people continue to suffer from PCS years after
444 their infection. Moreover, it is far from clear why some individuals recover spontaneously
445 over time, while others show no improvement, or worse, deteriorate.

446 Access to this large dataset has allowed us to explore neurophysiological differences between
447 individuals with post-COVID fatigue, according to the length of time individuals have been
448 affected by the condition. Within the first 6 months of having pCF, individuals already show a
449 number of changes in all three main divisions of the nervous system, in line with our previous
450 results[15]. People whose symptoms persist for longer than 6 months report significantly higher
451 levels of fatigue; this is corroborated by objective changes in peripheral muscle fatigue and
452 measures of cortical excitability and processing.

453 To assess overall physiological changes over time, the sum of Z scores across all measures was
454 taken. Individuals with pCF tended to have a higher sum than healthy controls ($p<0.001$;
455 Figure 4B) and there was a sharp incline between people having had pCF for three months
456 (definition of PCS according to NICE guidelines) to approximately one year (Figure 4A). Based
457 on this, we divided the pCF cohort into two distinct groups, in order to investigate which
458 measures were driving this worsening (diverging further away from healthy controls) over
459 time.

460 The first group contains people that have been affected by pCF for less than 200 days. When
461 comparing this cohort to healthy controls, we found evidence for autonomic dysfunction
462 (decreased blood oxygen saturation, increased heart rate and decreased heart rate
463 variability), increased peripheral muscle fatigue (*TI_PeriphFatigue*) and a reduction in intra-
464 cortical facilitation (*ICF*), a measure of intracortical glutamatergic function. There was also an
465 increase in body weight, though notably it was mainly the percentage of muscle mass that
466 appeared to increase.

467 These results largely replicate our previous findings[15], which included individuals that had pCF
468 for up to 179 days back in 2021. The addition of people that had pCF for less than 200 days,
469 but caught COVID roughly two years later in 2023, did not change these initial results, which
470 suggests that different virus variants have largely the same effect on pCF. The cohort of

individuals that had pCF for over 200 days at the time of testing includes people that were infected in late 2020 and up to early 2023. From alpha to omicron, the UK would have had 6 different virus variants during that time[35], with several subvariants. It is impossible to say for certain who caught which specific variant, therefore we cannot draw any conclusions on potential variant-specific effects.

People who continue to suffer from pCF after 200 days might reflect a group of true "long-haulers", with a spontaneous recovery becoming less likely after that time. These individuals report a significant increase in fatigue (FIS scores) compared to people that had pCF for a shorter amount of time. Objective measures support the fact that these individuals are left worse off over time, with several measures of cortical excitability and cognitive processing as well as peripheral muscle fatigue significantly changed after 200 days of pCF.

Neuromuscular fatigue is defined as a reduction in the capacity of muscles to generate force and has both peripheral and central origins. Peripheral fatigue reflects a failure of the peripheral nervous system, whereas central fatigue refers to the reduced ability of the central nervous system to activate muscles fully. During a sustained, fatiguing contraction, cortical excitatory drive increases in order to maintain force output, but inhibitory mechanisms such as intracortical inhibition and CSP concurrently intensify, resulting in an overall diminished corticospinal efficacy[36].

After 200 days of being affected by pCF, people show increased cortical excitability, with lower motor thresholds (*TMS_RMT, TMS_AMT, TMS_CSP_AMT*) and less stimulator intensity required to achieve 50% of both maximal MEP amplitude and maximal CSP duration (*TMS_I50, TMS_CSP_I50*), compared to individuals that had pCF for less than 200 days (Figure 5). Despite this cortical over-excitability, the cohort also had impaired central activation (*TI_CA_baseline, TI_CA_Fatigue*), indicating a deficit in the effectiveness of their cortical output.

This elevation of corticomotor excitability is likely a compensatory adjustment of the central motor networks, attempting to preserve force output despite reduced peripheral capacity to generate force. Peripheral myopathic changes are already apparent in individuals that had pCF for less than 200 days, whose muscles show a reduced ability to produce force in response

500 to electrical stimulation after a sustained contraction (*TI_PeriphFatigue*). This muscle fatigue
501 is further increased after 200 days of having pCF.

502 Emerging evidence suggests that mitochondrial dysfunction is a potential mechanism for
503 these changes. SARS-CoV-2 may impair mitochondrial function in muscles directly[37], even in
504 individuals suffering from PCS that have not been hospitalised[9,10]. Additionally, SARS-CoV-2
505 infection alters myokine signalling to sustain inflammation[38,39], which also impairs
506 mitochondrial function[40].

507 Individuals that had pCF for longer than 200 days also had significantly slower reaction times
508 (*STR_VART_Bic, STR_VART_1DI, STR_VSRT_Bic, STR_VSRT_1DI*), indicating diminished
509 cognitive processing[41], in line with increased cognitive fatigue.

510 Notably, none of the measures of autonomic function were different between the two pCF
511 cohorts. Autonomic dysregulation is a well-established feature of chronic fatigue[42] and
512 multiple studies indicate autonomic dysfunction after COVID-19[12,43-46]. Supporting this, we
513 found multiple abnormalities in autonomic function when comparing individuals with pCF to
514 healthy controls. Even before 200 days, people with pCF have reduced blood oxygen
515 saturation (*pO_2*), increased resting heart rate (*mean_HR*) and reduced heart rate variability
516 (*HR_RMSSD, pNN50*). While people affected by pCF for longer than 200 days also show
517 reduced blood oxygen saturation and heart rate variability (*HR_RMSSD, pNN50, HR_SDNN*),
518 surprisingly, their resting heart rate is lower than healthy controls, and habituation of their
519 galvanic skin response (GSR_Habituation) is increased (Figure 6B).

520 This suggests that while some dysautonomia is present both before and after 200 days of pCF,
521 it appears to remain stable, unlike measures of cortical excitability and cognitive processing,
522 which worsen over time. The changes in resting heart rate and galvanic skin response
523 habituation could reflect either a normalisation of underlying physiological function, or a
524 secondary compensatory process in which the primary pathology is masked by homeostatic
525 adjustments.

526 When looking at the distribution of the sum of Z scores over time, there is a drop between
527 360 and 800 days since infection, before it rises again to similar levels as the peak at 360 days
528 (Figure 4A). This pattern of rising and falling could imply a general fluctuation in symptom

529 burden, or perhaps this is a reflection of ongoing physiological adaptations. Longer follow up
530 studies are needed to determine how these trends continue after 1200 days.

531 In our previous longitudinal study[16], we followed 18 participants with pCF over 12 months
532 and found most neurophysiological metrics tended to return slowly to levels seen in healthy
533 controls, as well as participants reporting decreasing levels of fatigue. The progressive
534 normalization of aberrant measures, in parallel with improvements in Fatigue Impact Scores,
535 suggests that these changes arise as a consequence of a SARS-CoV-2 infection, rather than
536 reflecting a pre-existing phenotype predisposing individuals to develop post-COVID fatigue[16].

537 These observations, together with our findings here that people suffering from pCF for longer
538 show a general worsening of measures, indicates that while there is improvement over time
539 on an individual level, those people who remain fatigued beyond a critical time point develop
540 mal-adaptations (or perhaps fail to adapt) that contribute to them feeling physically,
541 cognitively and socially more fatigued than when the symptoms of post-COVID fatigue initially
542 emerged. A recent study by Taquet et al.[47] found very similar cognitive and psychiatric
543 symptom trajectories over 3 years. Their analysis of questionnaire scores concludes that
544 symptoms at 2-3 years were strongly predicted by the degree of recovery at 6 months, with
545 people with severe scores at 6 months very likely to experience an increase in symptom
546 burden over time. This further corroborates 6 months (~ 200 days) as the critical time point
547 beyond which accumulating physiological changes start to exacerbate PCS symptoms.

548 Our findings have implications for other studies aiming to investigate the mechanisms behind
549 post-COVID fatigue and the development of treatment approaches. Although we cannot say
550 what effects different variants or predispositions might have on the condition, it is evident
551 that people deviate physiologically based on how long they have been afflicted by pCF. This
552 could complicate comparative interpretation of different studies, since a pCF cohort meeting
553 the definition for pCF (3 months of persistent symptoms) potentially deviates significantly
554 from individuals with ongoing pCF over years. A key challenge for future trials will be to
555 balance recruitment to ensure even representation of pCF phenotypes. Without deliberate
556 stratification of symptom duration or physiological profile, treatment effects risk being
557 diluted or misinterpreted.

558

References

1 Maglietta, G. *et al.* Prognostic Factors for Post-COVID-19 Syndrome: A Systematic Review and Meta-Analysis. *J Clin Med* **11**, doi:10.3390/jcm11061541 (2022).

2 Office for National Statistics. (2023).

3 Hampshire, A. *et al.* Cognitive deficits in people who have recovered from COVID-19. *Eclinicalmedicine* **39**, doi:10.1016/j.eclinm.2021.101044 (2021).

4 Twomey, R. *et al.* Chronic Fatigue and Postexertional Malaise in People Living With Long COVID: An Observational Study. *Phys Ther* **102**, doi:10.1093/ptj/pzac005 (2022).

5 Carfi, A., Bernabei, R., Landi, F. & Gemelli Against, C.-P.-A. C. S. G. Persistent Symptoms in Patients After Acute COVID-19. *JAMA* **324**, 603-605, doi:10.1001/jama.2020.12603 (2020).

6 Groff, D. *et al.* Short-term and Long-term Rates of Postacute Sequelae of SARS-CoV-2 Infection: A Systematic Review. *JAMA Netw Open* **4**, e2128568, doi:10.1001/jamanetworkopen.2021.28568 (2021).

7 Goertz, Y. M. J. *et al.* Persistent symptoms 3 months after a SARS-CoV-2 infection: the post-COVID-19 syndrome? *ERJ Open Res* **6**, doi:10.1183/23120541.00542-2020 (2020).

8 Yong, S. J. Long COVID or post-COVID-19 syndrome: putative pathophysiology, risk factors, and treatments. *Infect Dis (Lond)* **53**, 737-754, doi:10.1080/23744235.2021.1924397 (2021).

9 Appelman, B. *et al.* Muscle abnormalities worsen after post-exertional malaise in long COVID. *Nat Commun* **15**, 17, doi:10.1038/s41467-023-44432-3 (2024).

10 Colosio, M. *et al.* Structural and functional impairments of skeletal muscle in patients with postacute sequelae of SARS-CoV-2 infection. *J Appl Physiol (1985)* **135**, 902-917, doi:10.1152/japplphysiol.00158.2023 (2023).

11 Krishna, B. A. *et al.* Spontaneous, persistent, T cell-dependent IFN-γ release in patients who progress to Long Covid. *Sci Adv* **10**, doi:10.1126/sciadv.adi9379 (2024).

12 Kurtoglu, E. *et al.* Altered cardiac autonomic function after recovery from COVID-19. *Ann Noninvasive Electrocardiol* **27**, e12916, doi:10.1111/anec.12916 (2022).

13 Wang, S., Quan, L. & Chavarro, J. E. Associations of Depression, Anxiety, Worry, Perceived Stress, and Loneliness Prior to Infection With Risk of Post-COVID-19 Conditions (Sept, 10.1001/jamapsychiatry.2022.2640, 2022). *Jama Psychiat* **79**, 1141-1141, doi:10.1001/jamapsychiatry.2022.3336 (2022).

14 Peter, R. S. *et al.* Post-acute sequelae of covid-19 six to 12 months after infection: population based study. *BMJ* **379**, e071050, doi:10.1136/bmj-2022-071050 (2022).

15 Baker, A. M. E. *et al.* Neural dysregulation in post-COVID fatigue. *Brain Commun* **5**, fcad122, doi:10.1093/braincomms/fcad122 (2023).

16 Maffitt, N. J. *et al.* Recovery of neurophysiological measures in post-COVID fatigue: a 12-month longitudinal follow-up study. *Sci Rep-Uk* **14**, doi:10.1038/s41598-024-59232-y (2024).

17 Fisk, J. D. *et al.* Measuring the Functional Impact of Fatigue - Initial Validation of the Fatigue Impact Scale. *Clin Infect Dis* **18**, S79-S83, doi:DOI 10.1093/clinids/18.Supplement_1.S79 (1994).

18 Sangari, S. & Perez, M. A. Imbalanced Corticospinal and Reticulospinal Contributions to Spasticity in Humans with Spinal Cord Injury. *J Neurosci* **39**, 7872-7881, doi:10.1523/JNEUROSCI.1106-19.2019 (2019).

19 Sangari, S., Lundell, H., Kirshblum, S. & Perez, M. A. Residual descending motor pathways influence spasticity after spinal cord injury. *Ann Neurol* **86**, 28-41, doi:10.1002/ana.25505 (2019).

20 Kujirai, T. *et al.* Corticocortical inhibition in human motor cortex. *J Physiol-London* **471**, 501-519, doi:10.1113/jphysiol.1993.sp019912 (1993).

21 McCleary, R. A. The nature of the galvanic skin response. *Psychological Bulletin* **47**, 97 (1950).

22 Walker, F. R. *et al.* Habituation of the electrodermal response - A biological correlate of resilience? *PLoS One* **14**, e0210078, doi:10.1371/journal.pone.0210078 (2019).

23 Fisher, K. M., Chinnery, P. F., Baker, S. N. & Baker, M. R. Enhanced reticulospinal output in patients with (REEP1) hereditary spastic paraplegia type 31. *J Neurol* **260**, 3182-3184, doi:10.1007/s00415-013-7178-6 (2013).

24 Dean, L. R. & Baker, S. N. Fractionation of muscle activity in rapid responses to startling cues. *J Neurophysiol* **117**, 1713-1719, doi:10.1152/jn.01009.2015 (2017).

25 Baker, S. N. & Perez, M. A. Reticulospinal Contributions to Gross Hand Function after Human Spinal Cord Injury. *J Neurosci* **37**, 9778-9784, doi:10.1523/JNEUROSCI.3368-16.2017 (2017).

26 Germann, M. & Baker, S. N. Evidence for Subcortical Plasticity after Paired Stimulation from a Wearable Device. *J Neurosci* **41**, 1418-1428, doi:10.1523/JNEUROSCI.1554-20.2020 (2021).

27 Logan, G. D. & Cowan, W. B. On the Ability to Inhibit Thought and Action - a Theory of an Act of Control. *Psychol Rev* **91**, 295-327, doi:Doi 10.1037/0033-295x.91.3.295 (1984).

28 Choudhury, S. *et al.* Slowed Movement Stopping in Parkinson's Disease and Focal Dystonia is Improved by Standard Treatment. *Sci Rep* **9**, 19504, doi:10.1038/s41598-019-55321-5 (2019).

29 McDonald, C., Newton, J., Lai, H. M., Baker, S. N. & Jones, D. E. Central nervous system dysfunction in primary biliary cirrhosis and its relationship to symptoms. *J Hepatol* **53**, 1095-1100, doi:10.1016/j.jhep.2010.05.036 (2010).

30 Benjamini, Y. & Hochberg, Y. Controlling the False Discovery Rate - a Practical and Powerful Approach to Multiple Testing. *J R Stat Soc B* **57**, 289-300, doi:DOI 10.1111/j.2517-6161.1995.tb02031.x (1995).

31 *Spider_plot*, <https://uk.mathworks.com/matlabcentral/fileexchange/59561-spider_plot> (2022).

32 Tapia, J. A., Tohyama, T., Poll, A. & Baker, S. N. The Existence of the StartReact Effect Implies Reticulospinal, Not Corticospinal, Inputs Dominate Drive to Motoneurons during Voluntary Movement. *J Neurosci* **42**, 7634-7647, doi:10.1523/JNEUROSCI.2473-21.2022 (2022).

33 Han, Q., Zheng, B., Daines, L. & Sheikh, A. Long-Term Sequelae of COVID-19: A Systematic Review and Meta-Analysis of One-Year Follow-Up Studies on Post-COVID Symptoms. *Pathogens* **11**, doi:10.3390/pathogens11020269 (2022).

34 Sudre, C. H. *et al.* Attributes and predictors of long COVID. *Nat Med* **27**, 626-631, doi:10.1038/s41591-021-01292-y (2021).

35 Lundberg, A. L. *et al.* Updated Surveillance Metrics and History of the COVID-19 Pandemic (2020-2023) in Europe: Longitudinal Trend Analysis. *JMIR Public Health Surveill* **10**, e53551, doi:10.2196/53551 (2024).
36 Taylor, J. L., Butler, J. E., Allen, G. M. & Gandevia, S. C. Changes in motor cortical excitability during human muscle fatigue. *J Physiol-London* **490 (Pt 2)**, 519-528, doi:10.1113/jphysiol.1996.sp021163 (1996).
37 Dodig, D. *et al.* COVID-19-Associated Critical Illness Myopathy with Direct Viral Effects. *Ann Neurol* **91**, 568-574, doi:10.1002/ana.26318 (2022).
38 Nigro, E. *et al.* Molecular mechanisms involved in the positive effects of physical activity on coping with COVID-19. *Eur J Appl Physiol* **120**, 2569-2582, doi:10.1007/s00421-020-04484-5 (2020).
39 Silva, C. C. *et al.* Muscle dysfunction in the long coronavirus disease 2019 syndrome: Pathogenesis and clinical approach. *Rev Med Virol* **32**, e2355, doi:10.1002/rmv.2355 (2022).
40 Georgieva, E. *et al.* COVID-19 Complications: Oxidative Stress, Inflammation, and Mitochondrial and Endothelial Dysfunction. *Int J Mol Sci* **24**, doi:10.3390/ijms241914876 (2023).
41 Cockshell, S. J. & Mathias, J. L. Cognitive functioning in chronic fatigue syndrome: a meta-analysis. *Psychol Med* **40**, 1253-1267, doi:10.1017/S0033291709992054 (2010).
42 Pagani, M. & Lucini, D. Chronic fatigue syndrome: a hypothesis focusing on the autonomic nervous system. *Clin Sci (Lond)* **96**, 117-125, doi:Doi 10.1042/Cs19980139 (1999).
43 Stahlberg, M. *et al.* Post-COVID-19 Tachycardia Syndrome: A Distinct Phenotype of Post-Acute COVID-19 Syndrome. *Am J Med* **134**, 1451-1456, doi:10.1016/j.amjmed.2021.07.004 (2021).
44 Blitshteyn, S. & Whitelaw, S. Postural orthostatic tachycardia syndrome (POTS) and other autonomic disorders after COVID-19 infection: a case series of 20 patients. *Immunol Res* **69**, 205-211, doi:10.1007/s12026-021-09185-5 (2021).
45 Rigo, S. *et al.* Impaired parasympathetic function in long-COVID postural orthostatic tachycardia syndrome - a case-control study. *Bioelectron Med* **9**, 19, doi:10.1186/s42234-023-00121-6 (2023).
46 Fedorowski, A. *et al.* Cardiorespiratory dysautonomia in post-COVID-19 condition: Manifestations, mechanisms and management. *J Intern Med* **294**, 548-562, doi:10.1111/joim.13652 (2023).
47 Taquet, M. *et al.* Cognitive and psychiatric symptom trajectories 2-3 years after hospital admission for COVID-19: a longitudinal, prospective cohort study in the UK. *Lancet Psychiat* **11**, 696-708, doi:10.1016/S2215-0366(24)00214-1 (2024).

Figures & Tables & Legends

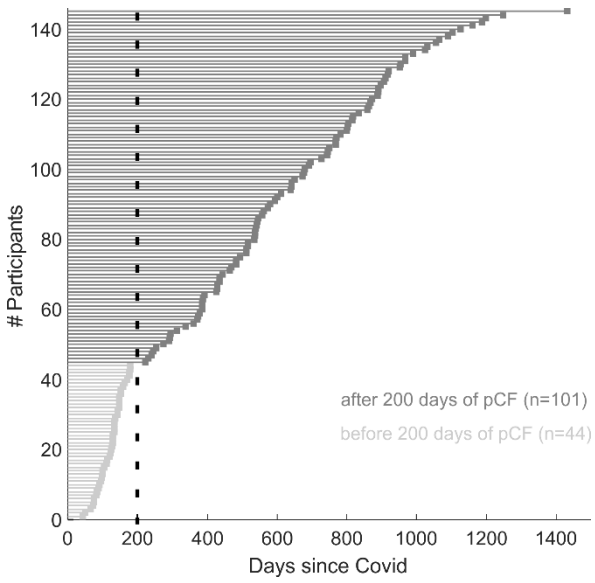

Figure 1: Distribution of time since SARS-CoV-2 infection which caused ongoing fatigue symptoms. *Light grey:* participants that had pCF for less than 200 days, *dark grey:* participants that had pCF for more than 200 days.

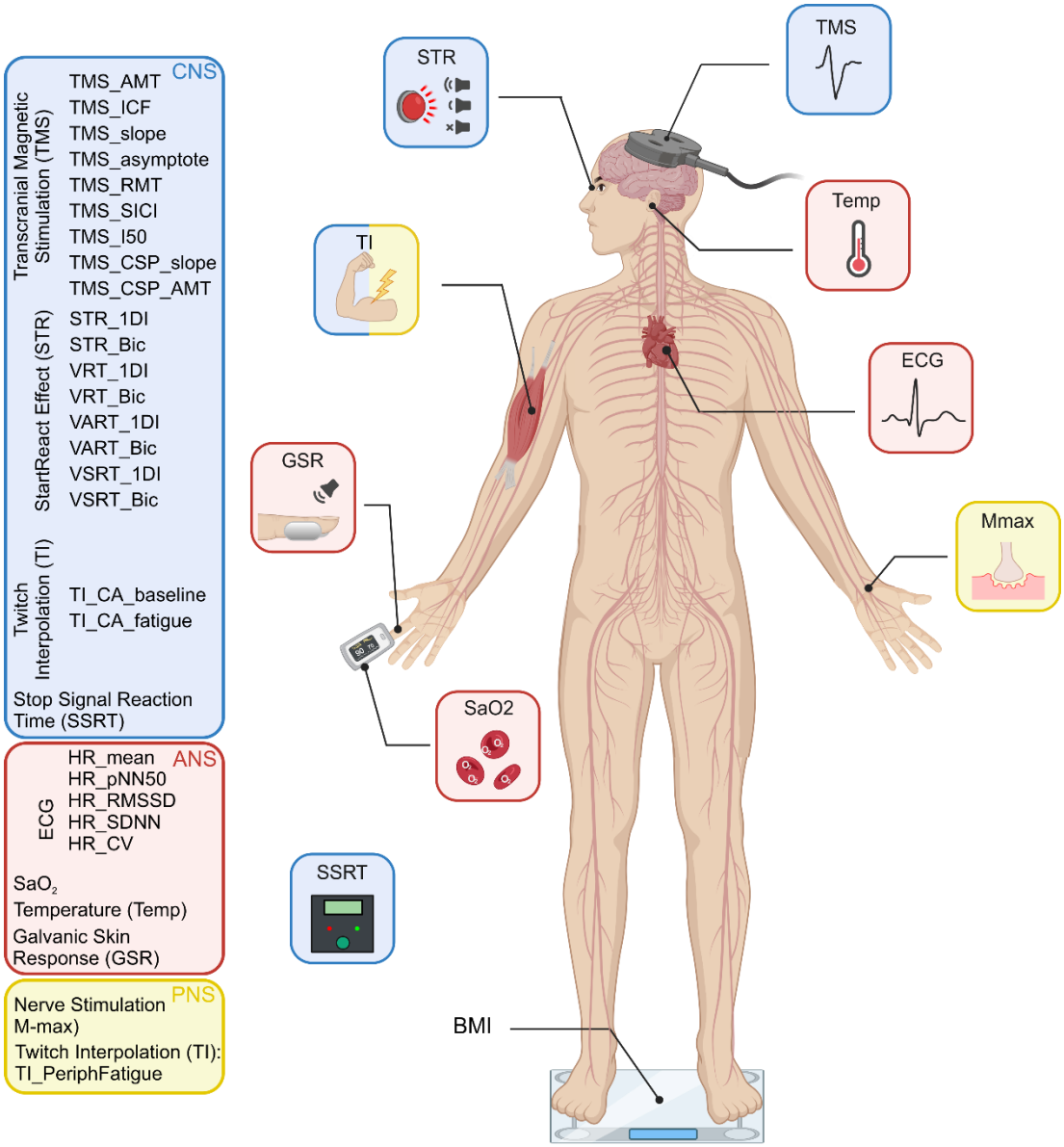

Figure 2: Schematic representation of the electrophysiological measures performed, separated according to which components of the nervous system (CNS, blue; PNS, yellow; and ANS, red) they assessed. Created with biorender.com.

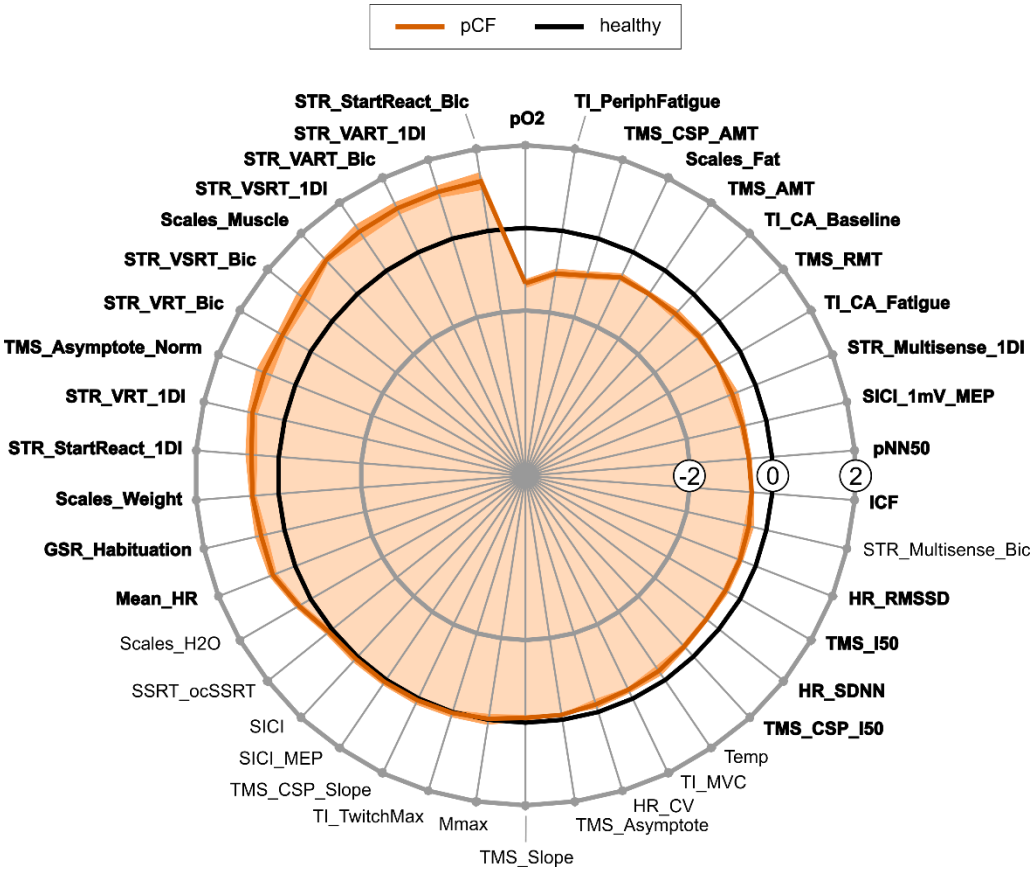

Figure 3: Comparison of pCF cohort with healthy controls. Data for each measure normalized as Z-scores (difference between pCF and control participants, scaled by SD). Black line at zero represents the control cohort, dark orange line the pCF cohort. Orange shading indicates the standard error of the mean difference (calculated by dividing the SD of each measure by the square root of the number of observations available). Measures are ordered so that the greatest difference is located at the top of the figure. Significant differences between the cohorts were assessed using unpaired t-tests. Measures passing the Benjamini-Hochberg correction for multiple comparisons are indicated in bold.

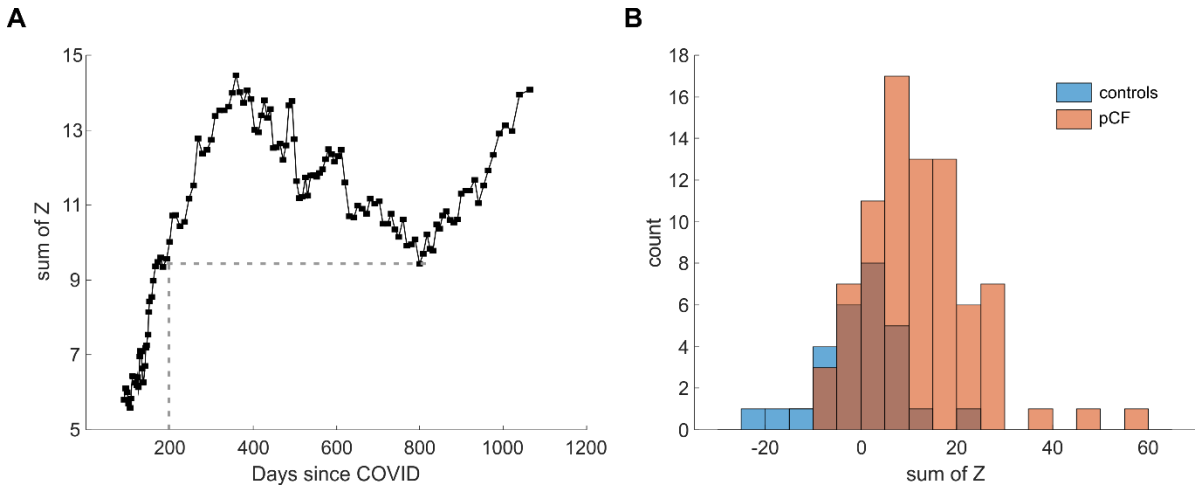

Figure 4: Distribution of sum of Z scores across all measures.

A: Each data point represents a bin of 20 subjects. Subjects were ranked in ascending order according to their time since infection (most recently infected to longest time since infection) and bins of 20 subjects were taken to contribute to the overall sum of Z score for that bin, starting with the 20 most recently infected people. Each bin was moved by one subject at a time until the last bin included the 20 subjects that had pCF for the longest. If participants did not have a measure, the missing data were substituted by the mean of the Z scores across all subjects for that measure. For the sum of Z scores to reflect overall symptom burden, the signage of measures where the mean of the pCF cohort was smaller than the mean of the healthy control cohort was flipped (multiplied by -1), so that a higher Z score always reflected a larger distance from healthy controls for all measures.

B: Sum of Z scores for each subject of the pCF (orange) and healthy control (blue) cohorts. The histogram has a bin width of 5.

FATIGUE IMPACT SCORE	All pCF vs healthy	< 200 days pCF vs healthy	> 200 days pCF vs healthy	Before vs after 200 days of pCF
FIS_total	-	-	-	**0.002**
FIS_social	-	-	-	**0.003**
FIS_physical	-	-	-	**0.006**
FIS_cognitive	-	-	-	**0.010**
CORTICAL				
SICI_RMT (%MSO)	**2.763×10^{-4}**	0.536	**1.071×10^{-6}**	**1.428×10^{-4}**
TMS_AMT (%MSO)	**5.887×10^{-7}**	0.091	**4.183×10^{-9}**	**6.328×10^{-5}**
TMS_I50 (%MSO)	**0.010**	0.629	**7.390×10^{-6}**	**3.451×10^{-6}**
TMS_asymptote (mV)	0.130	0.407	0.204	-
TMS_asymptote_norm (%Mmax)	**0.031**	0.115	**0.024**	0.322
TMS_slope (mV/%MSO)	0.385	0.658	0.380	-
TMS_CSP_AMT (ms)	**6.612×10^{-7}**	0.057	**4.117×10^{-9}**	**1.168×10^{-4}**
TMS_CSP_I50 (ms)	**0.013**	0.388	**3.935×10^{-6}**	**4.177×10^{-9}**
TMS_CSP_slope (ms/10%MSO)	0.782	0.329	0.820	-
SICI_ICF (%)	**4.795×10^{-5}**	**0.001**	**0.001**	0.353
SICI_SICI (%)	0.725	0.755	0.748	-
SICI_1mVMEP (%MSO)	**0.001**	0.628	**7.454×10^{-6}**	**4.225×10^{-4}**
SICI_MEP (mV)	0.768	0.757	0.612	-
TI_CA_baseline (%)	**0.002**	0.230	**0.001**	**0.018**
TI_CA_fatigued (%)	**4.005×10^{-6}**	0.036	**1.915×10^{-6}**	**0.006**
REACTION TIME				
STR_VRT_Bic (ms)	**0.001**	0.025	**3.591×10^{-4}**	0.163
STR_VRT_1DI (ms)	**4.604×10^{-4}**	0.017	**2.622×10^{-4}**	0.252
STR_VART_Bic (ms)	**3.056×10^{-5}**	0.022	**3.405×10^{-6}**	**0.008**
STR_VART_1DI (ms)	**7.676×10^{-6}**	0.011	**7.392×10^{-7}**	**0.010**
STR_VSRT_Bic (ms)	**0.003**	0.274	**0.001**	**0.015**
STR_VSRT_1DI (ms)	**4.778×10^{-4}**	0.070	**7.387×10^{-5}**	**0.021**
STR_Multisens_Bic (ms)	0.042	0.818	**3.447×10^{-4}**	-
STR_Multisens_1DI (ms)	**0.017**	0.945	**2.084×10^{-5}**	**0.003**
STR_StartReact_Bic (ms)	**0.001**	0.015	**2.962×10^{-4}**	0.462
STR_StartReact_1DI (ms)	**0.009**	0.091	**0.003**	0.525
SSRT_ocSSRT (ms)	0.614	0.262	0.926	-
PERIPHERAL				
TI_PeriphFatigue (%)	**2.928×10^{-7}**	**0.007**	**1.488×10^{-8}**	**0.009**
TI_MVC (N)	0.090	0.298	0.095	-
TI_TwitchMax (N)	0.838	0.035	0.492	-
NMJ_Mmax (mV)	0.919	0.359	0.809	-
AUTONOMIC				
Mean_HR (Hz)	**0.003**	**0.001**	**0.018**	0.060
HR_RMSSD (ms)	**0.007**	**0.007**	**0.027**	0.347
HR_SDNN (ms)	**0.004**	0.015	**0.012**	0.488
pNN50 (%ge)	**8.246×10^{-6}**	**0.008**	**1.315×10^{-5}**	0.505
HR_CV (Ratio)	0.305	0.362	0.331	-
pO2 (%)	**1.419×10^{-10}**	**2.881×10^{-7}**	**1.431×10^{-9}**	0.917
GSR_Hab (Habituation %)	**0.022**	0.068	**0.021**	0.786
Temp (Co)	0.272	0.057	0.044	-
BODY COMPOSITION				
Scales_Weight (kg)	**4.247×10^{-4}**	**1.441×10^{-4}**	**0.004**	0.064
Scales_Muscle (kg)	**3.416×10^{-10}**	**3.770×10^{-5}**	**1.959×10^{-10}**	0.306
Scales_Fat (%)	**1.157×10^{-4}**	0.374	**1.025×10^{-6}**	**2.858×10^{-4}**
Scales_H2O (%)	0.045	0.984	**0.006**	-

742

Table 1: List of p values for each measure comparing the whole pCF cohort (n=145) to the healthy control (n=52) cohort (left column), people who had pCF for less than 200 days (n=44) to healthy controls (middle left column), people who had pCF for over 200 days (n=101) to healthy controls (middle right column) and the two pCF cohorts to each other (right column). Measures between cohorts were compared with unpaired t-tests. Significant p-values that passed correction for multiple comparisons are marked in bold. P-values that were significant but did not pass correction for multiple comparisons are marked in grey. Unit of measure is given in brackets.

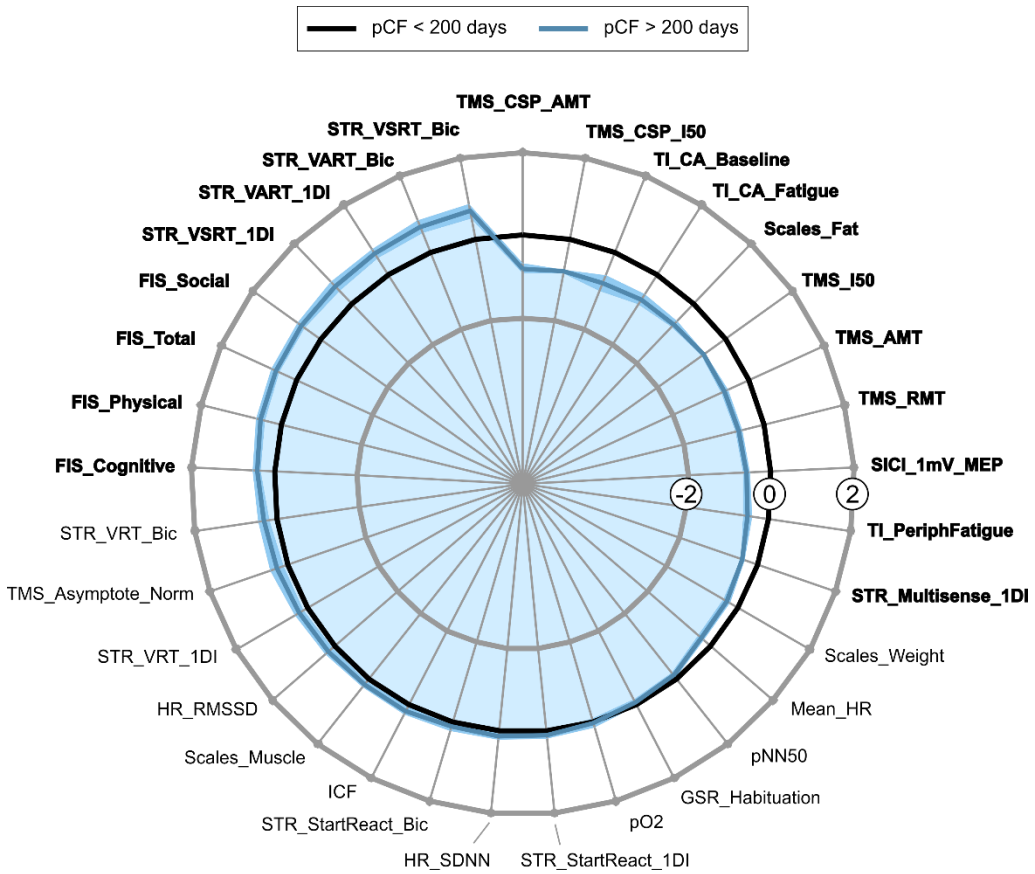

Figure 5: Comparison of participants that had pCF for less than 200 days (black) and over 200 days (blue). Data for each measure normalized as Z-scores. Black line at zero represents the pCF cohort whose infection was less than 200 days ago, dark blue line the pCF cohort who was infected over 200 days ago. Blue shading indicates the standard error of the mean difference (calculated by dividing the SD of each measure by the square root of the number of observations available). Measures are ordered so that the greatest difference is located at the top of the figure. Significant differences between the cohorts were assessed using unpaired t-tests. Measures passing the Benjamini-Hochberg correction for multiple comparisons are indicated in bold.

A

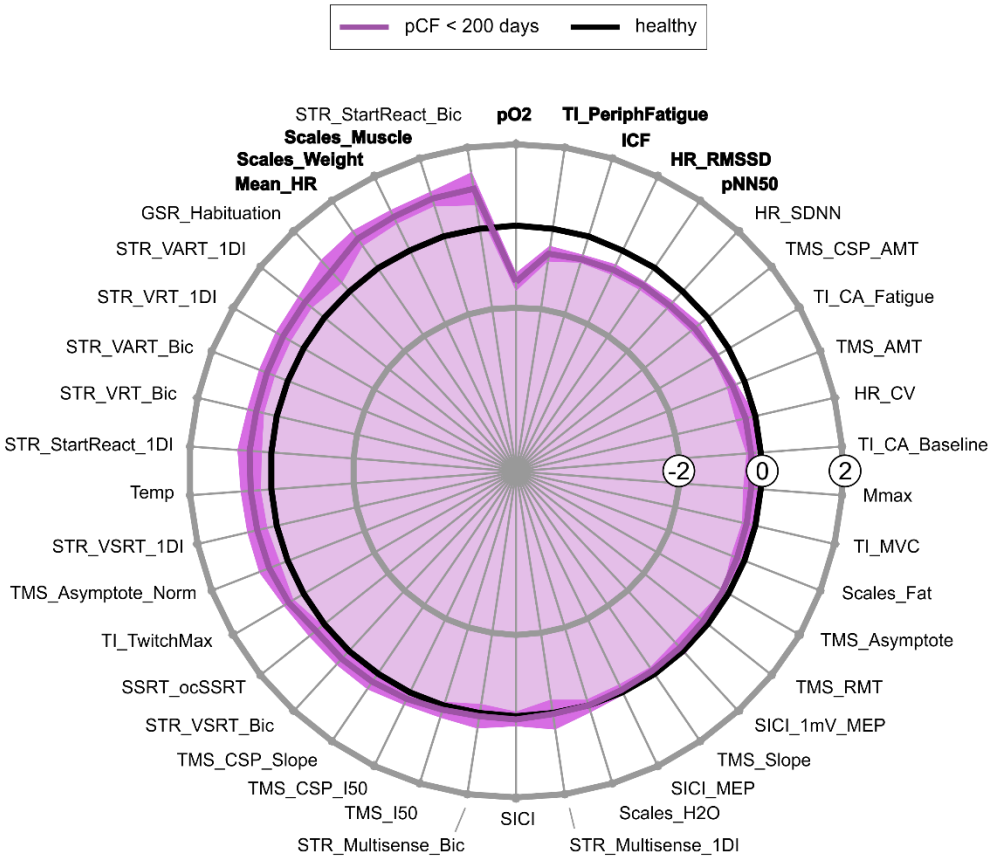
pCF < 200 days
healthy
STR_StartReact_Bic
pO2
TI_PeriphFatigue
Scales_Muscle
ICF
Scales_Weight
HR_RMSSD
Mean_HR
pNN50
GSR_Habituation
HR_SDNN
STR_VART_1DI
TMS_CSP_AMT
STR_VRT_1DI
TI_CA_Fatigue
STR_VART_Bic
TMS_AMT
STR_VRT_Bic
HR_CV
STR_StartReact_1DI
TI_CA_Baseline
Temp
-2
0
2
Mmax
STR_VSRT_1DI
TI_MVC
TMS_Asymptote_Norm
Scales_Fat
TI_TwitchMax
TMS_Asymptote
SSRT_ocSSRT
TMS_RMT
STR_VSRT_Bic
SICI_1mV_MEP
TMS_CSP_Slope
TMS_Slope
TMS_CSP_I50
SICI_MEP
TMS_I50
SICI
Scales_H2O
STR_Multisense_Bic
STR_Multisense_1DI

B

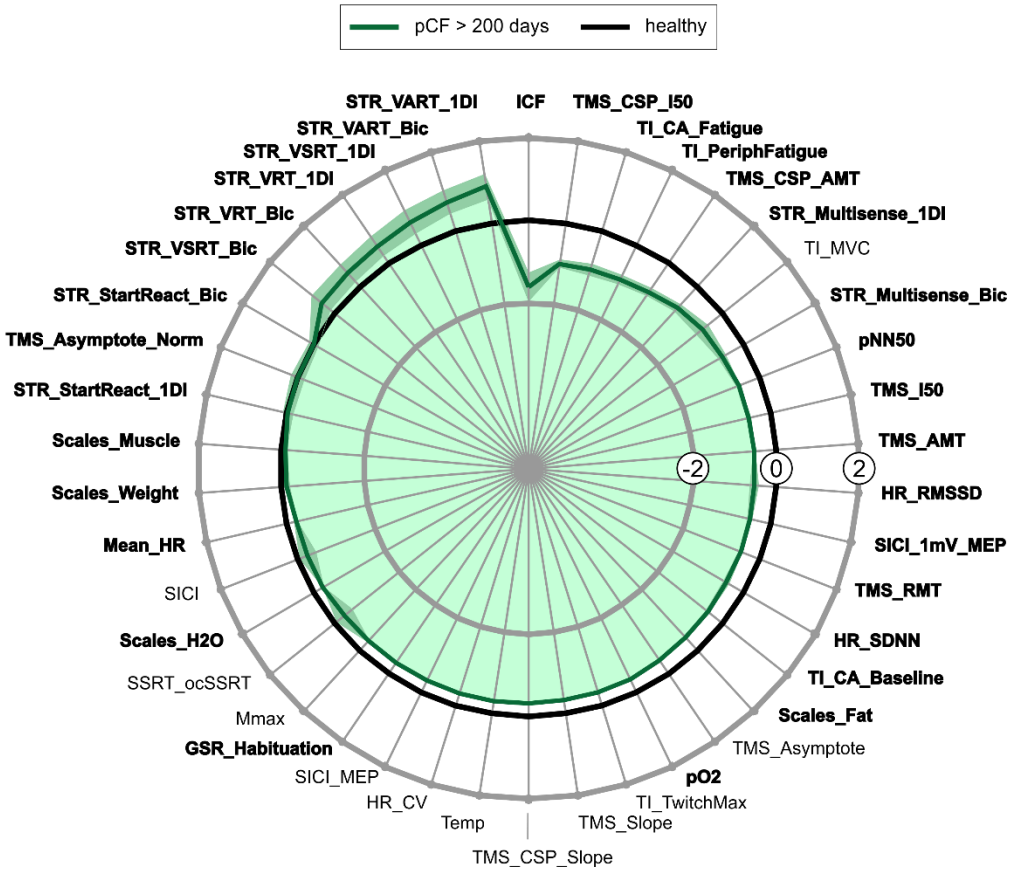
pCF > 200 days
healthy
STR_VART_1DI
ICF
TMS_CSP_I50
STR_VART_Bic
TI_CA_Fatigue
STR_VSRT_1DI
TI_PeriphFatigue
STR_VRT_1DI
TMS_CSP_AMT
STR_VRT_Bic
STR_Multisense_1DI
STR_VSRT_Bic
TI_MVC
STR_StartReact_Bic
STR_Multisense_Bic
TMS_Asymptote_Norm
pNN50
STR_StartReact_1DI
TMS_I50
Scales_Muscle
TMS_AMT
-2
0
2
Scales_Weight
HR_RMSSD
Mean_HR
SICI_1mV_MEP
SICI
TMS_RMT
Scales_H2O
HR_SDNN
SSRT_ocSSRT
TI_CA_Baseline
Mmax
Scales_Fat
GSR_Habituation
TMS_Asymptote
SICI_MEP
pO2
HR_CV
TI_TwitchMax
Temp
TMS_Slope
TMS_CSP_Slope

781

Figure 6: Comparison of the two pCF cohorts with healthy controls. Data for each measure are normalized as Z-scores. Measures are ordered so that the greatest difference is located at the top of the figure. Significant differences between the cohorts were assessed using unpaired t-tests. Measures passing the Benjamini-Hochberg correction for multiple comparisons are indicated in bold. **A:** Black line at zero represents the control cohort, dark purple line the pCF cohort who was infected less than 200 days ago. Purple shading indicates the standard error of the mean difference. **B:** Black line at zero represents the control cohort, dark green line the pCF cohort for whom the index infection occurred over 200 days before recruitment. Green shading indicates the standard error of the mean difference.